Process Safety and Environmental Protection 183 (2024) 203–216

Contents lists available at ScienceDirect

Process Safety and Environmental Protection

journal homepage: www.journals.elsevier.com/process-safety-and-environmental-protection

Consequences of subsea CO_2 blowouts in shallow water

Federica Tamburini, Sarah Bonvicini, Valerio Cozzani *

LISES – Laboratory of Industrial Safety and Environmental Sustainability, DICAM - Department of Civil, Chemical, Environmental and Materials Engineering, University of Bologna, via Terracini 28, 40131 Bologna, Italy

ARTICLE INFO

Keywords:
CCUS
Blowout
Subsea CO_2 storage
Submarine plume
Surfacing gas
Atmospheric dispersion
Threshold distances

ABSTRACT

Safety and risk assessment of the offshore geological storage of carbon dioxide (CO_2) in the Carbon Capture, Utilization, and Storage (CCUS) value chain needs the evaluation of the consequences of possible accidental submarine CO_2 leakages, including releases having high flow rate and very long duration, as blowouts. An innovative procedure for the estimation of the effects of submarine blowouts in shallow water was developed, based on the integration of specific sub-models. A model for blowout simulation is used to predict the features of the source term. The fate of the submarine plume is then assessed. Finally, the atmospheric dispersion of the surfacing gas is simulated, to estimate damage distances. The application of the methodology to a set of case studies evidences that in extremely shallow water the threshold distances of the gas cloud dispersing in the air can be higher for CO_2 than for natural gas. However, when considering higher water depths, the release of CO_2 to the atmosphere is strongly attenuated by the dissolution of CO_2 in the water column.

1. Introduction

In the framework of the energy transition, Carbon Capture, Utilization, and Storage (CCUS) shall provide a valuable contribution to the sustainable reduction of carbon dioxide (CO_2) emissions to the atmosphere in hard-to-abate applications (IEA, 2021, 2020; Koornneef et al., 2010).

Within the CCUS chain, geological storage is proposed for the long-term storage of CO_2. Although, in general terms, permanent storage can occur either onshore or offshore, the latter case - which includes saline aquifers and depleted oil and gas reservoirs - is the most attractive for several European countries due to the greater capacity available at sea (EC, 2011; IPCC, 2005). Focusing on Europe, in the North Sea region several CCUS projects involve CO_2 storage into saline aquifers (BEIS, 2021; Chadwick and Eiken, 2013; Equinor, 2019a). Differently, in the Adriatic Sea interest in storing CO_2 in depleted natural gas reservoirs seems more attractive. Actually, adapting or even reusing existing infrastructures originally installed for the production of natural gas allows for a reduction in both the costs and the environmental impact of such projects (ENI, 2020). Moreover, exhausted hydrocarbon reservoirs are appealing storage sites also due to the presence of an extended geological characterization of the reservoirs obtained from the previous exploration and production activities (Hoteit et al., 2019).

The geological storage of CO_2 poses significant safety issues, both during the injection phase and in the long term, due to the possibility of leakages (Directive, 2009/31/EC, 2009; Papanikolaou et al., 2011). When considering injection into offshore sites, the risk of accidents causing submarine CO_2 releases is of particular relevance, because of the severe operating conditions and the large amounts of CO_2 potentially involved (ClimateWise, 2012). Since there is historical evidence of natural gas blowouts from production wells (DNV, 2017; Holand, 1997; Li et al., 2019; SINTEF, 2021), the occurrence of CO_2 blowouts from injection wells is deemed possible (Blackford et al., 2012; ETIP ZEP, 2019). Actually, blowout accidents are extremely hazardous scenarios, usually characterized by high release rates and very long durations (ClimateWise, 2012; Jewell and Senior, 2012). These characteristics make them potentially capable of causing considerable damage in relation to specific targets (e.g., humans, assets, or the environment). Therefore, to assess the impact posed by such events, specific approaches to risk estimation must be implemented. Keeping in mind that the risk depends on the likelihood and the severity of the consequences of damage events (Directive 2009/31/EC, 2009), assessing the risk from subsea blowouts implies evaluating the occurrence frequencies and effects of such accidents.

Scarce data are available concerning the likelihood and expected frequencies of CO_2 blowout scenarios. Actually, the limited operating experience available for marine CCUS does not allow the derivation of specific CO_2 leakage frequencies. Therefore, on the one hand, in several

* Corresponding author.
E-mail address: valerio.cozzani@unibo.it (V. Cozzani).

https://doi.org/10.1016/j.psep.2024.01.008
Received 30 October 2023; Received in revised form 18 December 2023; Accepted 2 January 2024
Available online 5 January 2024

technical documents the similarity between natural gas and CO_2 blowouts is remarked, thus suggesting to derive frequency values for CO_2 blowouts from those available for natural gas blowouts, mostly resulting from past accident data (IOGP, 2019; Jordan and Benson, 2008; Porse et al., 2014). On the other hand, the few available papers addressing the consequences of CO_2 blowouts focus mostly on the modelling of the dispersion of the CO_2 plume in the water column, with limited attention to the possibility of a CO_2 plume forming on sea surface and dispersing in the atmosphere (Dissanayake et al., 2021; Oldenburg and Pan, 2020, 2019).

In the framework of offshore CCUS projects considering sequestration in exhausted natural gas reservoirs, the investigation of the similarities and the differences between natural gas and CO_2 submarine leakages is of utmost interest. Actually, a huge experience is present in managing the risk and in assessing the consequences of natural gas blowouts. Obtaining a higher understanding of the analogies and differences between CO_2 and natural gas releases thus allows the enhancement of current knowledge concerning CO_2 blowouts, including risk assessment studies and management practices. This is even more important when threshold distances are considered, since the extension of the potential impact area of accidental releases may affect the possibility to operate in specific exploitation areas, as well as the reuse and/or adaptation of offshore natural gas infrastructures to CO_2 transport and injection.

The differences in the chemical and physical properties of CO_2 and natural gas, as well as in their inherent hazardous characteristics, do not allow a straightforward comparison of their consequences in case of submarine leakages. In fact, while the solubility in water of methane (CH_4) and of the other hydrocarbons composing natural gas is rather low, CO_2 solubility in water is relevant (Weiss, 1974; Yamamoto et al., 1976). Hence, the flux of gaseous CO_2 emerging at the sea surface can be much lower than the CO_2 blowout rate, since CO_2 is in part absorbed into the water column (Lian et al., 2022; Olsen and Skjetne, 2020). Furthermore, owing to their different densities, the plume formed by natural gas behaves as a light gas after being released into the atmosphere, while CO_2 disperses as a heavy plume (HSE, 2009; Li et al., 2018b). From the point of view of the hazardous properties, natural gas is a flammable mixture, while airborne CO_2 is a mildly toxic gas (Equinor, 2019b; Harper et al., 2011; Xing et al., 2013). In addition, because of the acid-base reactions taking place between dissolved CO_2 and water (known as the “carbonate system reactions” (Glade and Al-Rawajfeh, 2008)), the dissolution of CO_2 in water results in a reduction in the pH of seawater (Lian et al., 2022). This acidification of the marine environment may harm the marine biota living in the water column and on the seafloor (Jones et al., 2015; Lian et al., 2022; Widdicombe et al., 2015, 2009). Thus, specific approaches and models are sorely needed to assess and compare the consequences and the potential damage of CO_2 releases with respect to those of natural gas.

In the present study, a novel approach was developed to provide a comprehensive model capable of predicting the consequences of subsea blowouts. Three sub-models were integrated, each originally conceived for an independent use, respectively addressing blowout rate calculation, CO_2 water plume dispersion and CO_2 atmospheric dispersion. The integrated methodology developed provides a comprehensive and straightforward approach to the calculation of the consequences of offshore CO_2 blowouts, that may affect the safety and environmental impact of Carbon Capture and Storage projects. Actually, the original results obtained allow the assessment of the formerly largely unknown impact profile of offshore CO_2 blowouts, for which limited evidence is present in the literature. The results thus allow for the first time a comparative assessment among the consequences of CO_2 and those of natural gas offshore blowouts. In particular, threshold distances for damage to humans on the sea surface obtained for offshore blowouts of CO_2 and natural gas were obtained and compared, allowing a better understanding of CO_2 blowouts impact profile, that is extremely important in the context of risk assessment of CCS technologies.

The following part of the paper is organized as follows. In Section 2, the integrated methodology developed for the evaluation of the consequences of subsea blowouts is presented, also describing the specific sub-models necessary for its application. Section 3 introduces a set of case studies used to test the procedure and show its strengths. Results are presented in Section 4 and discussed in Section 5. Finally, some conclusive remarks are drawn in Section 6.

2. Methods and models

The developed procedure consists of three integrated and sequential steps:

1. blowout modelling and characterization, by a geological reservoir - wellbore model;
2. modelling of the submarine plume generated by the blowout, to obtain the gas flow released in the atmosphere at the sea surface;
3. modelling of the atmospheric dispersion of the gaseous plume above the sea surface.

In Fig. 1, the procedure is schematized along with the inputs and outputs of the sub-models proposed for each step, discussed in the following.

2.1. Simulation of the blowout

A blowout is a transient multi-component and multi-phase non-isothermal flow from the reservoir (which can be described as a porous medium) through the wellbore up to the wellhead. The blowout flow rate depends on a broad spectrum of factors related to the geological features of the reservoir, the geometrical and operational data of the wellbore, and the thermodynamic properties of the spilled fluid (Norwegian Oil and Gas Association, 2021). Several models and software tools are available to estimate the blowout flow rate, such as the freely available T2Well code (Pan and Oldenburg, 2014), the commercial software tool LedaFlow (Kongsberg Digital, 2023), and the Drillbench Blowout Control code powered by the OLGA simulator (Schlumberger, 2023). All these tools provide the mass flow rate over time of each component in each phase, as well as the pressure and temperature at the point of leakage. Typically, steady-state conditions take over shortly after the release begins. Therefore, the description of the fate of the spill (in the water column first, then in the atmosphere) was carried out considering a constant outflow term (Oldenburg and Pan, 2020; Olsen and Skjetne, 2016). Additionally, while in natural gas blowouts, CH_4 and the other light hydrocarbons are always in the gas phase, in the case of CO_2 blowouts, both gaseous and liquid CO_2 are released during the transient phase after the start of the blowout. However, the flux of liquid CO_2 decreases with time, thus, when the steady-state is reached, the flow rate (which is sub-sonic) involves only gaseous CO_2 (Oldenburg and Pan, 2020).

Overall, in this stage of the procedure a model able to simulate the blowout rate from the reservoir was applied to provide the release rate of the reservoir fluid, thus allowing the characterization of the source term (i.e., outflow rate, pressure, temperature, etc.). Geological features of the reservoir, wellbore parameters and specific assumptions concerning the blowout scenario also need to be input to the model. One of the software tools mentioned above may be selected and applied to carry out the simulation. As an example, the application of the T2Well code to simulate offshore and onshore CO_2 well blowouts has been described by (Oldenburg and Pan, 2019).

2.2. Simulation of the submarine plume

In case of blowouts occurring on the seafloor, the high momentum of the release determines the formation of a gas bubble plume generated by the outflowing jet. Usually, for the sake of simplicity, models neglect

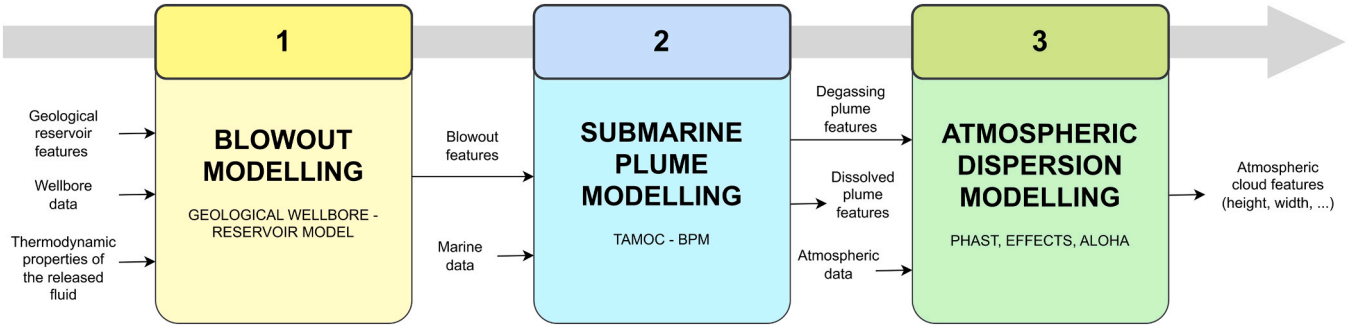

Fig. 1. Scheme of the integrated procedure developed in the present study and of the specific tools considered to carry out each step.

local phenomena affecting the near-field of the outlet flow and assume a horizontal outflow section, so that initially the jet has a vertical orientation and high speed. However, sea currents incline its axis and interfacial drag forces slow down its velocity (Socolofsky et al., 2015).

The physics of gas releases in shallow water has been discussed extensively elsewhere (Olsen and Skjetne, 2016). Herein, it is sufficient to mention that the blowout flow, immediately after the release section, breaks up into bubbles, which rise due to both the initial momentum of the release and buoyancy, as shown in Fig. 2. The turbulence of the ascending bubbles causes the entrainment of seawater into the plume. Along their upward path, CO_2 bubbles may in part dissolve into water. The bubbles that reach the sea surface are released into the atmosphere, while the seawater entrained in the plume is diverted into a radial flow just below the sea surface, outwards from the plume eye (see Fig. 2-a)). It is also possible for the released CO_2 to dissolve completely before the gas bubbles reach the surface. If dissolution completes just below the sea surface, the plume of entrained water and dissolved CO_2 turns into a radial flow once it reaches the sea surface (Fig. 2-b)). If dissolution completes well below the sea surface, when neutral buoyancy is achieved the plume bends horizontally due to the action of currents (see Fig. 2-d)). Alternatively, depending on the intensity of the cross currents, these may bend the plume in the downstream direction so that the gaseous plume remains somehow trapped in the water column. However, the largest bubbles may still escape from the upper edge of the trapped plume, continuing to ascend toward the sea surface (see Fig. 2-c)).

For the simulation of the submarine plume, Computational Fluid Dynamic (CFD) modelling can be applied, solving the full transient and three-dimensional Navier-Stokes equations, which express the conservation of mass, momentum, and energy. The continuous improvements in the availability of computing resources and the development of numerical methods make the use of CFD increasingly affordable, allowing the simulation of the main features of subsea gas releases in good accordance with experimental data (Geng et al., 2021; Li and Wang, 2023; Olsen and Skjetne, 2016; Sun et al., 2020). In fact, CFD models can accurately simulate the trajectories of the CO_2 plume dispersing in the ocean, providing highly resolved profiles of the concentration of CO_2 dissolved in the seawater and the fraction of CO_2 degassing at the sea surface (Cloete et al., 2009; Li et al., 2018a; Pham et al., 2020).

A review of CFD models developed for the description of submarine CO_2 plumes has been presented in (Pham et al., 2020), while examples of the application of CFD models in the context of risk assessment of gaseous submarine releases have been reported in the literature (Equinor, 2019b; Ulfsnes et al., 2013). The numerical CFD codes which appear to be used most frequently are Ansys Fluent (Ansys, 2023a) and Ansys CFX (Ansys, 2023b). However, the absence of validation data is a critical issue that affects the application of CFD models to subsea blowouts. Indeed, while several datasets are available for low-speed CO_2 seepages from the seabed, few experiments have been conducted to date to simulate and analyse high-velocity submarine CO_2 releases (Roberts and Stalker, 2020).

As an alternative to CFD models, integral models can be adopted for the description of the plume. In this case, the conservation equations, i.e., the mass, momentum, and energy balances, are solved along the differential horizontal slices of the plume, taking into account water entrainment and introducing basic plume velocity and concentration profiles obtained from simplified empirical models (Li et al., 2018a; Socolofsky et al., 2008; Socolofsky and Bhaumik, 2008). Among this category of models, the Texas A&M Oilspill Calculator (TAMOC) is a freely available modelling suite, developed for the reproduction of wide ranges of subsea single- and multi-phase spills, assuming steady-state conditions. The TAMOC suite includes the Bent Plume Model (BPM) module for the simulation of blowouts (Dissanayake et al., 2018; Socolofsky et al., 2015; TAMOC, 2023), which combines the dynamic equations of motion with detailed equations of state, needed to capture the thermodynamic properties of the fluids, the phase equilibria, the dissolution process, and the buoyancy effects (Gros et al., 2018). Originally developed to model oil blowouts (Gros et al., 2017), the TAMOC - BPM code can now handle also gaseous releases and the presence of a background cross current (Oldenburg and Pan, 2020).

Fig. 3 shows a scheme of the input and output data of the TAMOC - BPM code. The TAMOC - BPM code considers the jet as formed by bubbles of different diameters, d_i. A specific module determines the median bubble diameter d_{50} as a function of the blowout features (i.e., diameter, flow rate, temperature, and pressure). Then, a further module estimates the probability distribution of the bubble diameters around the median value.

The core model of the TAMOC - BPM code, taking as input the blowout diameter and flow rate, the environmental data, and the distribution of the bubble size, simulates the behaviour of the plume. The output includes the gas flow emerging into the atmosphere and that dissolving in the water column, the entrained water flow, the plume semi-width on the sea surface, and the surfacing time of the gas bubbles (Dissanayake et al., 2018; Socolofsky et al., 2015).

In the present study, the TAMOC - BPM code was used to perform the second step of the simulation, as it allows a straightforward assessment of the plume features and of the CO_2 dissolution in water, requiring much less computational resources than CFD models. Although integral models have inherent limitations compared to CFD models, the absence of extended validation data sets, in particular for the description of the jet in the flow establishment zone, limits the potentially higher accuracy of CFD simulations. Moreover, it is important to highlight that the near-field dispersion of the gas jet simulated by means of CFD or integral models needs to be coupled with the simulation of the dispersion of the CO_2-enriched water in the far-field (i.e., at a regional scale, in basin wide domains). For this purpose, models for the simulation of ocean hydrodynamics are needed (Amir Rashidi et al., 2020; Blackford et al., 2020, 2013). Currently, such models experience limitations in considering the input data from the near-field modelling, thus not being able to take advantage of a more detailed simulation of the near-field dispersion as that obtained by CFD simulations with respect to integral models (Dewar et al., 2014).

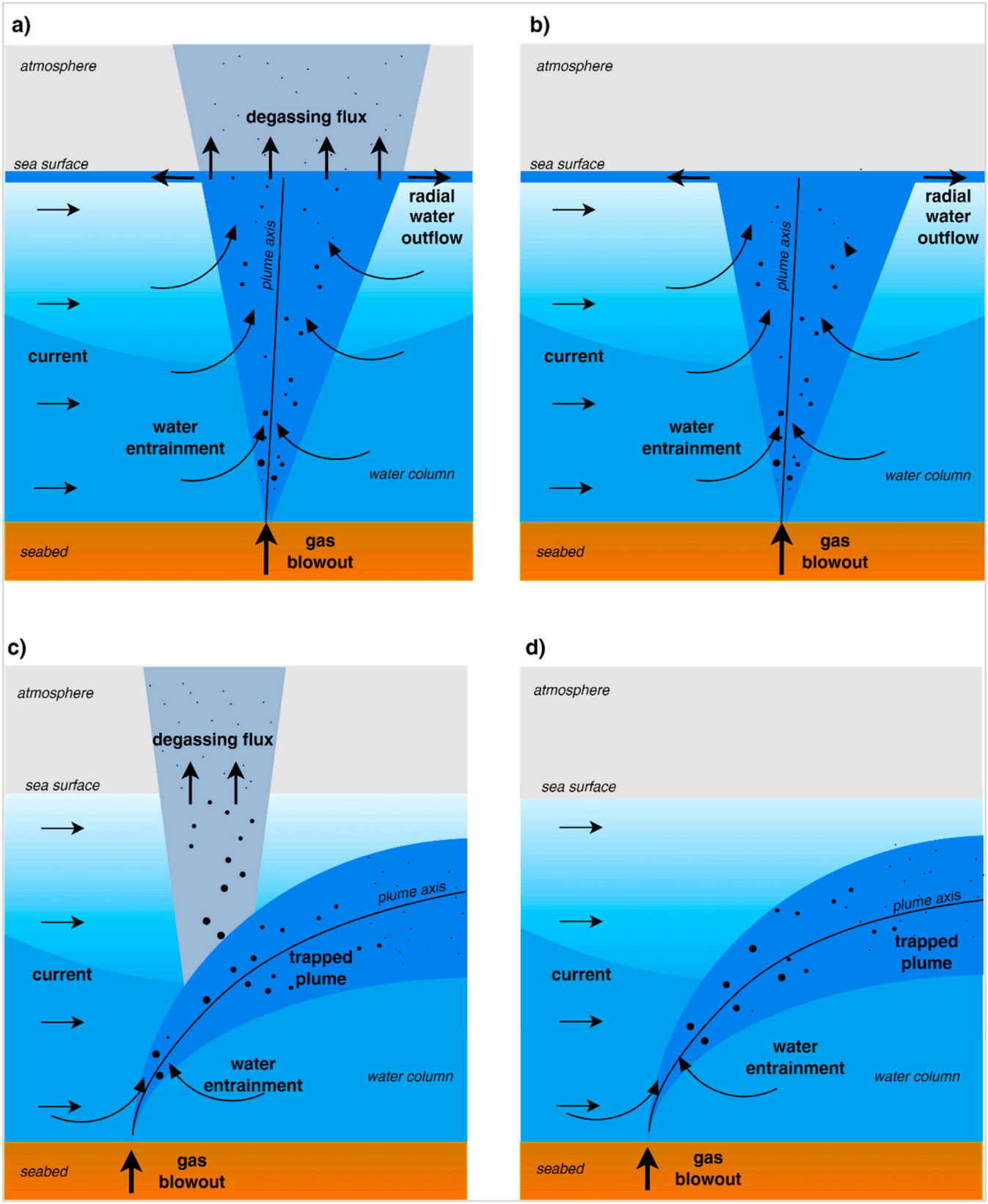

Fig. 2. Schematization of a gaseous submarine jet formed by a gas blowout at the sea bottom: a) gas partly dissolves in water and partly escapes in the atmosphere, while the entrained seawater flows out radially below the sea surface; b) gas completely dissolves in water and the entrained seawater flows radially below the sea surface; c) the gas plume is trapped in the water column with only the bigger gas bubbles reaching the sea surface; d) the gas plume is trapped in the water column with no gas bubbles reaching the sea surface.

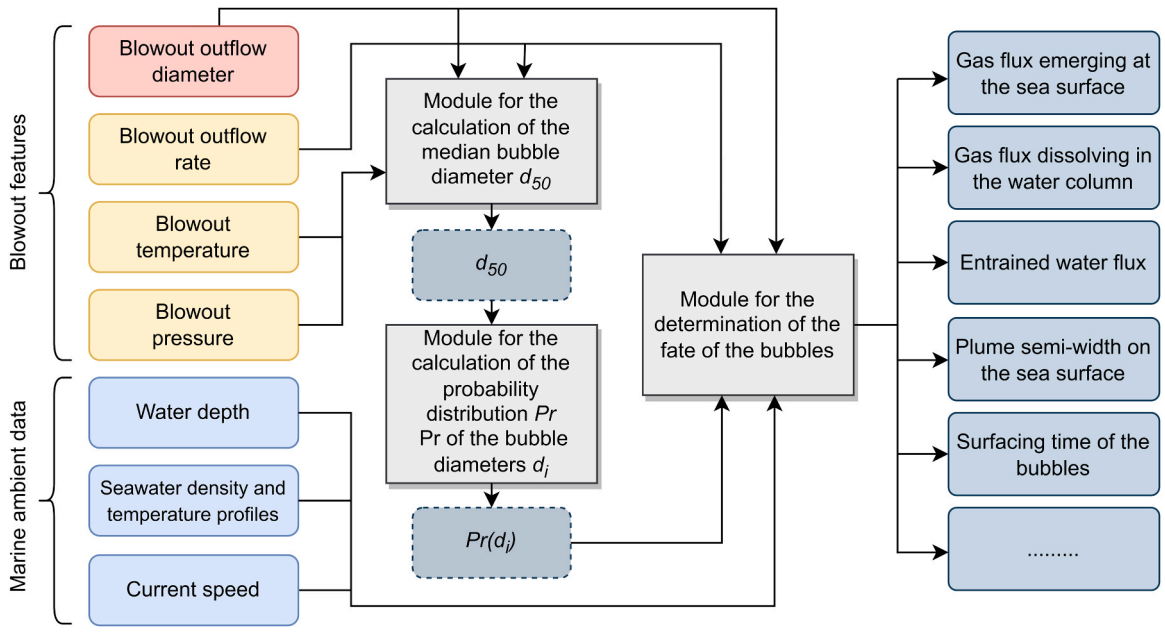

Fig. 3. Flow diagram of the TAMOC - BPM code showing the input data and the main results.

2.3. Simulation of the atmospheric dispersion

Natural gas and CO_2 disperse in the air both passively, under the action of wind and atmospheric turbulence, and actively, due to gravitational effects associated with their densities, which differ from that of air. The criterion adopted for distinguishing between passive or non-passive dispersion is the critical Richardson's Number (Ri_c), assessed in case of continuous or semi-continuous release sources. When considering CH_4, that is usually the main component of natural gas, its density at 15 °C is equal to 0.7 kg/m^3 (i.e., nearly the half of that of air, which is 1.2 kg/m^3) and the Ri_c value is lower than 1, thus the gas plume is considered passive. Contrarily, in the same conditions, CO_2 is characterized by a density of 1.9 kg/m^3, about 1.5 higher than that of air. The Ri_c in case of CO_2 dispersion is higher than 1, thus CO_2 disperses as a heavy gas (Engineering Toolboox, 2023). The different behaviour of the two gas plumes leaving the water surface is schematized in Fig. 4.

In the case of natural gas, besides the dispersion scenario, in the presence of ignition sources, the possibility of both Vapour Cloud Fire (VCF) and Vapour Cloud Explosion (VCE) must be considered. In virtue of the low reactivity of natural gas, however, it should be remarked that a VCE is only possible in case the plume engulfs a fixed or floating offshore structure (Sponge, 1999).

To calculate the threshold distances for humans of the airborne plumes of natural gas and CO_2, it was necessary to identify some hazard thresholds of the two substances. For flammable gases, threshold values were derived from the Lower Flammability Limit (LFL or 0.5LFL) and were usually considered for the Vapour Cloud Fire (Haynes, 2014), while blast wave maximum overpressures were proposed for the Vapour Cloud Explosion (D.M. 09.05.2001, 2001). For toxic gases, several parameters can be adopted as thresholds for potential damage to humans,

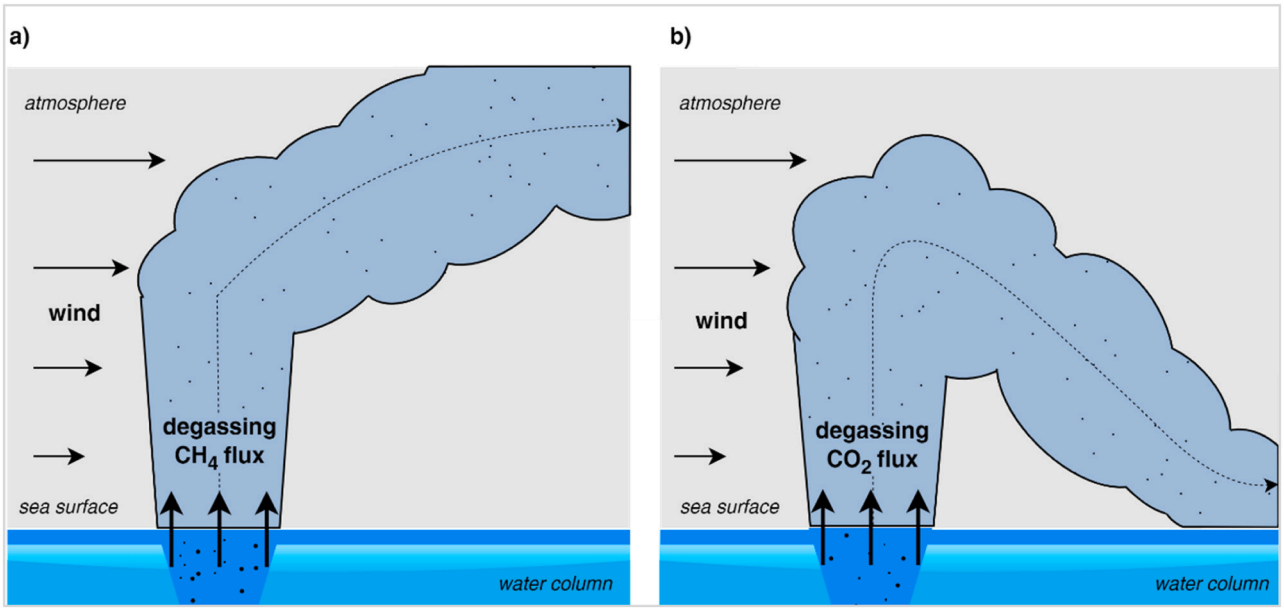

Fig. 4. Schematization of the dispersion of the gas emerging from the water column: a) natural gas plume in air; b) CO_2 plume in air.

as the Significant Likelihood Of Death (SLOD) concentration, also called Lethal Concentration (LC), referred to a death probability of 50% after an inhalation exposure of 30 min, and the Immediately Dangerous to Life and Health (IDLH) limit (Harper et al., 2011; NIOSH, 2007).

With the aim of comparing the threshold distances of accidental scenarios involving flammable and toxic substances, in land-use planning practices equivalent doses or thresholds of the physical effects associated to fires, explosions, and toxic clouds are frequently used. In the present approach, the thresholds reported in Table 1 were applied, derived from the Italian Decree on land use planning around Seveso sites (D.M. 09.05.2001, 2001). With respect to natural gas, the table reports the threshold values available for CH_4. However, the threshold values for any specific natural gas composition may be easily calculated by well-established procedures (Mannan, 2012).

CFD codes, integral models, and simplified tools can be adopted to simulate the dispersion of the gas plume leaving the sea surface. Depending on the type of model adopted, different accuracies can be achieved in the dispersion predictions. Integral and simplified models result in lower accuracy with respect to CFD code, in particular in the near field, due to the implementation of assumptions required to handle complex local phenomena (Sherpa Consulting, 2015). A comprehensive review of the strengths and drawbacks of CFD and integral approaches to the atmospheric dispersion of CO_2 is presented in (Sherpa Consulting, 2015), while a comparison of the threshold distances provided by CFD and integral models can be found in (Gant et al., 2014). Regarding simplified tools, it is worth mentioning that a nomogram-based procedure for the atmospheric dispersion of CO_2 has recently been developed (Oldenburg and Zhang, 2022; Zhang et al., 2016). However, this tool is not able to simulate the dispersion of light plumes. Among the CFD codes, Ansys Fluent (Ansys, 2023a), Ansys CFX (Ansys, 2023b), DNV KFX (DNV, 2023a), Fluidyn PANACHE (Fluidyn, 2023), GEXCON FLACS-CFD (Gexcon, 2023a), and OpenFOAM (OpenC.F.D. Ltd, 2023) have been applied for the simulation of CO_2 plumes dispersing in the air (Sherpa Consulting, 2015).

The absence of obstacles on the sea surface and the ability of some integral tools to consider the formation of atmospheric plumes from wide area allow the use of this category of models to assess the damage distances of the CO_2 and natural gas plumes formed by subsea blowouts (Witlox et al., 2017). In the framework of integral models, ALOHA by the United States Environmental Protection Agency (US EPA) (US EPA, 2023), PHAST by Det Norske Veritas (DNV) (DNV, 2023b), and EFFECTS by GEXCON (Gexcon, 2023b) have to be mentioned. These tools present specific differences when applied for the simulation of the dispersion of the degassing flux of submarine blowouts, as reported in Table 2. In particular, the ALOHA code considers only point sources and neglects the velocity of the release. This is an important limitation in the framework of the present study. Actually, as shown in Fig. 2 and Fig. 4, the degassing flux emerges from a wide area at sea surface. Moreover, when the submarine plume reaches the sea surface (see Fig. 2-a)), the gas can enter the atmosphere at a significant speed.

When considering the velocity of the release, it is necessary to point out that also the EFFECTS software (version 12), despite having some options for the dispersion of light gases, is not able to model jet releases of light gases. Consequently, among the above cited integral models, only the PHAST software can be used for the comparison of the degassing flux threshold distances of natural gas and CO_2 blowouts.

Therefore, based on the aforementioned considerations, in the methodology developed the PHAST software was selected as the more suitable tool to simulate the atmospheric dispersion of CO_2 and natural gas on the sea surface.

Table 1
Physical effects thresholds for damage to humans applied in the present study for CH_4 and CO_2.

Substance	Scenario	Human Health Endpoints *ppm*		References
		Lethal effects	*Irreversible injuries*	
CH_4	VCF - Vapour Cloud Fire	50000 (LFL)	25000 (0.5LFL)	(Haynes, 2014)
	VCE - Vapour Cloud Explosion	0.3 bar	0.07 bar	(D.M. 09.05.2001, 2001)
CO_2	Toxic cloud dispersion	92000 (LC_{50})	40000 (IDLH)	(Harper et al., 2011; NIOSH, 2007)

Table 2
Main differences in the features of the integral models included in the ALOHA, PHAST, EFFECTS software codes affecting the simulation of the atmospheric dispersion of the degassing flux.

Feature		Software code and version		
		ALOHA *5.4.7*	PHAST *8.4*	EFFECTS *12*
Type of gas	light	✓	✓	✓
	neutral	✓	✓	✓
	heavy	✓	✓	✓
Characterisation of the outflowsource	effective dimensions of the outflow section	X	✓	✓
	speed of the outflow	X	✓	only for heavy gases
	orientation of the outflow section	X	✓	✓

3. Case studies

A set of notional case studies consisting in CO_2 and natural gas blowout scenarios is presented to show the application of the procedure described above. The investigated releases are supposed to occur from gas reservoirs in shallow waters, as those present in the North Adriatic Sea, with seabed depth ranging from − 10 m to − 80 m (W.M.S. GEBCO, 2023; WebGIS UNMIG, 2023).

Natural gas is a complex mixture of hydrocarbons and other species, whose composition may be extremely different in different reservoirs. However, the predominant component of natural gas is usually CH_4. Moreover, CH_4 is the hydrocarbon component of natural gas having the lower molecular weight, thus it is expected to show the highest differences with respect CO_2 when considering atmospheric dispersion. Thus, in the framework of the notional test cases carried out in the present study, natural gas is assumed to be composed only of CH_4.

With regard to the blowout rate, in order to compare the severity of the consequences of CO_2 and CH_4 releases from a specific gas reservoir, it would be necessary to compare (i) the maximum foreseeable outflow rate from the production well during reservoir exploitation for CH_4 and (ii) the maximum foreseeable outflow rate from the same well used as the injection well for the submarine CO_2 storage in the case of CO_2. However, the operational conditions of a reservoir, on which the maximum blowout rate depends, are generally different during natural gas production and during the CO_2 injection (e.g., in terms of pressure, temperature, and gas saturation). Hence, even if the geometrical features of the wellbore are the same during both operations, due to the differences in the thermodynamic properties of the two substances and the operational conditions of the reservoir, different outflow rate values would be obtained when simulating the blowout by means of the methods described in Section 2.1. For the sake of clarity and of brevity, the detailed modelling of the reservoir and the blowout rate is thus out of scope of the analysis of the notional case studies. The reader is addressed to literature publications exemplifying the application of the consolidated models used for blowout modelling (e.g., see Oldenburg and Pan, 2019 and reference cited therein).

Therefore, in the framework of the notional test cases carried out in the present study, in order to compare the consequences of natural gas and CO_2 blowouts, the source term is defined on the basis of literature data (Blackford et al., 2009; Olsen and Skjetne, 2016). More specifically, five different release rate values in the range 100 ÷ 300 kg/s are assumed for both CH_4 and CO_2 blowouts. These flow rates correspond to rather severe blowouts, which can originate from a release pressure of about 40 bar, a temperature of 10 °C and an equivalent release diameter of about 150 mm (Blackford et al., 2009; Olsen and Skjetne, 2016).

The selected outflow rates are input to the TAMOC - BPM code (version 2.4.0), that is then applied to simulate the submarine dispersion of the gas plume (Step 2 of the methodology), as discussed above. In the application of the software, the initial median diameter of the gas bubbles d_{50} is set equal to 5 mm for CH_4 blowouts and to 0.5 mm for CO_2 blowouts. These values are selected on the basis of the results provided by the TAMOC - BPM module for the calculation of the median bubble diameter and are validated through experimental results reported in the literature (Gros et al., 2019; Sellami et al., 2015). The probability distribution of the gas bubble diameters is generated by a specific module of the TAMOC - BPM code, as shown in Fig. 3. More specifically, the probability distribution is calculated for 10 diameter values d_i adopting the experimental Rosin-Rammler distribution (Wang et al., 2018). Annual average profiles of seawater temperature and density along the water column are determined using a literature correlation (Crounse, 2000) and temperature, pressure, and salinity profiles in the North Adriatic Sea reported by (Artegiani et al., 1997) are assumed. A depth-averaged crossflow current equal to 0.15 m/s is considered (Bolaños et al., 2014).

In Step 3 of the methodology, the PHAST software (version 8.4) is applied to simulate CH_4 and CO_2 dispersions in the atmosphere. In the case of CO_2, simulations are obtained using also the ALOHA (version 5.4.7) and EFFECTS (version 12) software packages for the sake of comparison.

Typical yearly averaged values for the North Adriatic Sea are considered for air temperature and relative humidity values (Meteo Areonautica Militare, 2023), while Pasquill class F and wind speed of 2 m/s are assumed to provide a conservative evaluation of the threshold distances. A summary of the main environmental data used in the case studies analysis is reported in Table 3.

4. Results

4.1. Submarine bubble plume

Fig. 5 reports different mass flow rates of CO_2 and CH_4 as a function of the seafloor depth of the blowout, for the blowout scenarios described in Section 3. In particular, Fig. 5-a) shows that the CO_2 flow rate emitted at the sea surface decreases as the seafloor depth of the blowout increases, due to the dissolution of CO_2 in the water column, as highlighted in (Oldenburg and Pan, 2020). This behaviour completely differs from that of CH_4, as shown in Fig. 5-b), where the flow rates of CO_2 and

Table 3
Environmental data assumed for the simulation of the case studies.

Marine data			
Seawater temperature	°C	13 (at depth − 80 m) ÷ 17 (at depth − 10 m)	
Seawater density	kg/m^3	1030 (at depth − 80 m) ÷ 1027 (at depth − 10 m)	
Sea current	m/s	0.15	
Atmospheric data			
Air temperature		°C	15
Relative humidity		%	70
Pasquill class		-	F
Wind speed		m/s	2 (at 10 m above sea level)

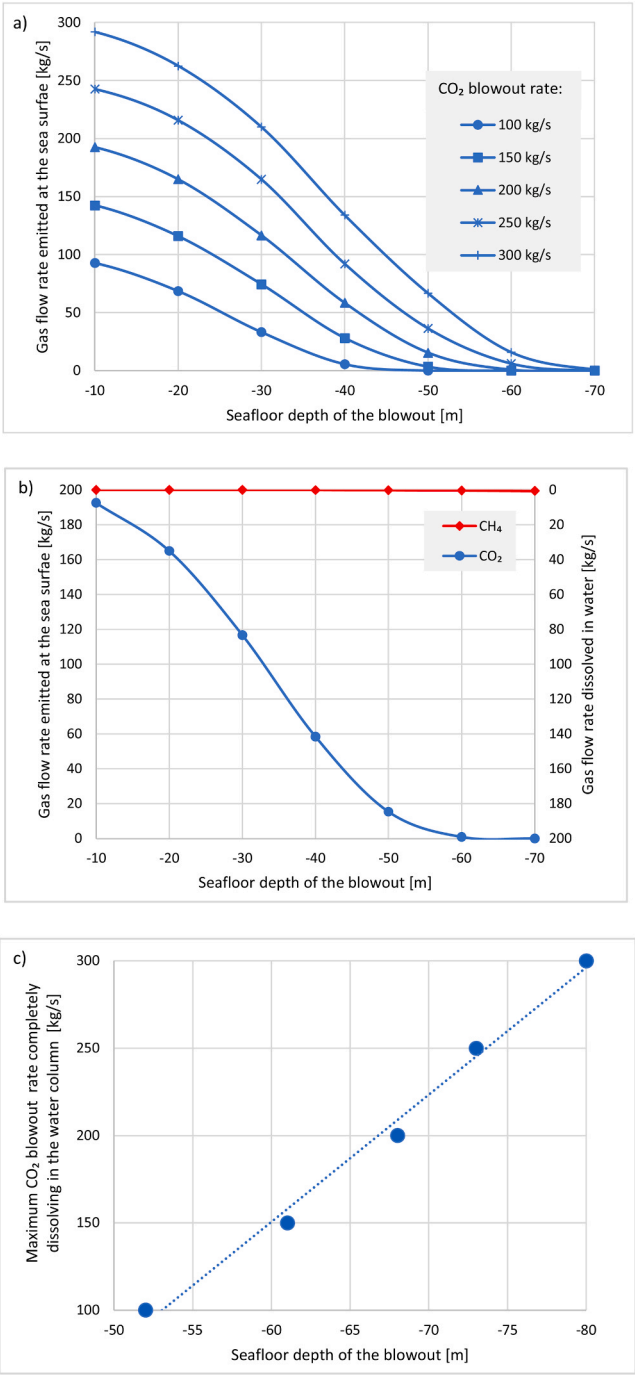

Fig. 5. Mass flow rates of CH_4 and CO_2 as a function of the seafloor depth of the blowout: a) flow rate of CO_2 emitted at the sea surface for different blowout rates; b) comparison of the flow rates of CO_2 and CH_4 emitted at the sea surface and dissolved in water for the 200 kg/s blowout; c) maximum CO_2 blowout rate completely dissolving in the water column.

CH_4 leaving the sea surface and dissolving in water are compared in the case of a blowout rate of 200 kg/s. In fact, it can be noticed that the amount of CH_4 dissolved in water is almost negligible. Lastly, Fig. 5-c) reports the maximum CO_2 blowout rate completely dissolving in the water column for different seafloor depths of the blowout. It can be noticed that, at seafloor depths below − 80 m, there is no CO_2 emerging into the air for all the blowout rates considered. Fig. 5-c) also evidences a roughly linear trend of the maximum CO_2 blowout rate completely dissolving in the water column with respect to seafloor depth of the blowout.

A further important difference is present between the behaviour of CO_2 and CH_4 following a subsea release. As shown in Fig. 6, a longer time is required by the CO_2 bubbles to reach the sea surface with respect to CH_4 bubbles. This result derives from the lower outflow speed of CO_2 from the well and from the larger surface area of the CO_2 bubbles (due to their smaller median diameter): e.g., for the 200 kg/s blowout occurring at a seafloor depth of − 50 m, the discharge velocity of CO_2 is three times lower with respect to the one of CH_4.

The geometrical features of the CH_4 and CO_2 bubble plumes in the water column are compared in Fig. 7, considering blowouts occurring at different seafloor depths. Although the figure only reports the results obtained for the blowout rate of 200 kg/s, qualitatively similar results were obtained for all outflow rates. The outcomes evidence that the CH_4 and CO_2 plumes have nearly identical shapes and sizes for all the seabed depths considered. In all cases, independently from the substance, the plume centrelines are slightly deflected from the vertical direction by the crossflow current. However, the inclination is barely perceptible, due to the difference of three orders of magnitude between the rising velocity of the gaseous bubbles and the speed of the current, assumed equal to 0.15 m/s.

It should also be remarked that the presence of CO_2 gaseous bubbles in the water plume reduce its overall apparent density. Therefore, in the specific scenarios analyzed, no descending plumes are formed.

Still with respect to the 200 kg/s blowouts, CH_4 forms an atmospheric plume whatever the seafloor depth, thus its behaviour is well represented by Fig. 2-a). In contrast, CO_2 emerges from the seawater only for the blowouts that occur at seafloor depths lower than around − 65 m (see Fig. 7-a), -b) and -c)). In these cases, their behaviour is represented by Fig. 2-a), as for CH_4. In case of the CO_2 blowout occurring at − 70 m (see Fig. 7-d)), Fig. 2-b) best approximates its behaviour. Indeed, in the case of this CO_2 blowout, coherently with the absence of a degassing flow evidenced in Fig. 5-b) and Fig. 5-c), the CO_2 bubbles completely dissolve immediately below the sea surface. Thus, the plume of entrained water and dissolved CO_2 turns into a radial flow once it reaches the sea surface, as shown in Fig. 8, but no atmospheric plume is formed.

As a further result, the width of the bubble plume on the sea surface is shown in Fig. 9 for the case studies corresponding to a blowout rate of 200 kg/s. It can be noticed that the plume width values increase almost linearly with the seafloor depth of the blowout.

With respect to the results reported in Fig. 9, it should be highlighted that the presence of gaseous bubbles reduces the overall density of the water plume. This phenomenon is of great concern when degassing occurs, as it may potentially cause the sinking of ships, even if the drag force of the upward flow of entrained water could partially compensate for the effects of the density modification (Beegle-Krause and Lynch, 2005; Hueschen, 2010; Li et al., 2019, 2018b; Ruppel et al., 2008). Actually, Fig. 10 shows that relevant fluxes of water are entrained in the subsea bubble plume formed as a consequence of a blowout. The seawater entrainment rate is higher for natural gas blowouts than for CO_2 blowouts. This behaviour reflects the trend of the outflow speed from the well, which is higher for natural gas blowout scenarios.

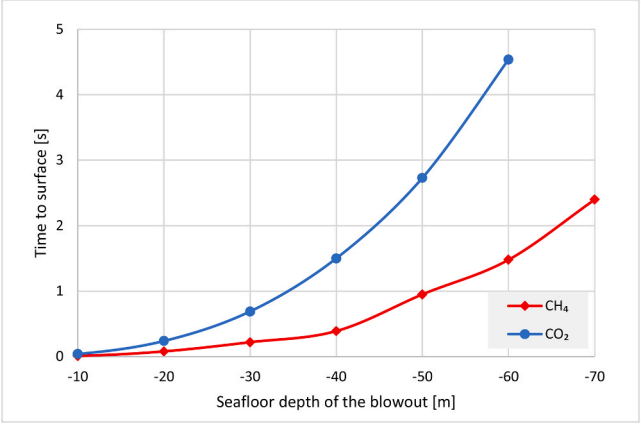

Fig. 6. Surfacing time of CH_4 and CO_2 gas bubbles for the 200 kg/s blowouts as a function of the seafloor depth of the blowout.

4.2. Atmospheric dispersion

In order to simulate the atmospheric dispersion of the degassing flow formed from subsea gas releases, it is important to consider that a circular area is formed on the sea surface where the gas bubbles emerge forming an atmospheric plume. The diameter of the area corresponds to the bubble plume width on the sea surface. Therefore, it depends on the depth of the seabed where the blowout takes place.

Considering the case studies defined in Section 3, assuming a 200 kg/s blowout rate and a seafloor depth of − 10 m, in the case of CH_4, the flow rate of the gas leaving the sea surface is almost equal to that released at the seafloor, emerging from a circular area of 1.7 m radius, as shown in Fig. 7 and Fig. 9. Instead, when considering CO_2, the flow rate at the sea surface is slightly lower due to the dissolution in water (the dissolved flow rate is about 193 kg/s) and the radius of the emerging area equals 1.6 m. As expected, Fig. 7 and Fig. 9 evidence that the deeper the seafloor depth where the blowout takes place, the wider the area of the degassing surface and the lower the degassing velocity of CH_4 or CO_2 bubbles at the sea surface. For CO_2 blowouts, it should also be considered that the degassing flux decreases when the depth of the seabed increases.

The velocity of the emerging gas bubbles may be non-negligible, depending on the conditions of the release. Assuming a density of 0.7 kg/m^3 for CH_4 bubbles at the sea surface, a value of 32 m/s may be assumed as a rough estimate of the average velocity, obtained dividing the volumetric flow rate by the extent of the plume section at the sea surface. In the case of CO_2, a similar calculation provides a value of 13 m/s, much lower than that of CH_4 due to the higher density of CO_2 (1.9 kg/m^3). Since the average degassing velocity can assume high values, up to one order of magnitude higher than the wind speed, the adoption of an atmospheric dispersion model able to simulate a jet release is required, so to take into account the spill rate, the surfacing area, the speed of the release, and its orientation.

The PHAST software (DNV, 2023b) was used to simulate the atmospheric dispersion of the vertical jet releases of CH_4 and CO_2 obtained for the blowouts assumed as case studies. Fig. 11 reports the downwind threshold distances calculated for the case studies corresponding to a blowout rate of 200 kg/s. In particular, Fig. 11 includes the threshold distances for the VCF (corresponding to the LFL and 0.5LFL concentration thresholds), for the VCE (corresponding to specific blast wave peak overpressure limits) and for the toxic dispersion (corresponding to the LC_{50} and IDLH concentration thresholds). The threshold distances represent maximum values over the vertical direction. It should be believed that these values may occur at different heights above the sea surface, due to the different shapes of the CH_4 and CO_2 plumes shown in Fig. 4. Moreover, for the sake of simplicity, the threshold distances of the VCE were estimated using the TNT model (The Netherlands Organization of Applied Scientific Research, 2005), thus they represent a first estimate, to be refined by applying more sophisticated VCE models.

Fig. 11-a) shows that, as expected, in the case of CH_4 the potential threshold distances of the VCE are more than double those of the VCF. Additionally, for both the VCF and the VCE, the threshold distances are nearly independent from the seafloor depth. This is due to the negligible absorption of CH_4 along the water column during bubble rise and the mutual compensation of two factors influenced by the depth of the seabed: the extension of the degassing area and the average velocity of the gas at the sea surface. As discussed above, the former increases with the seafloor depth, while the latter decreases. In the case of CO_2, as shown in Fig. 11-b), the threshold distances increase when the seabed

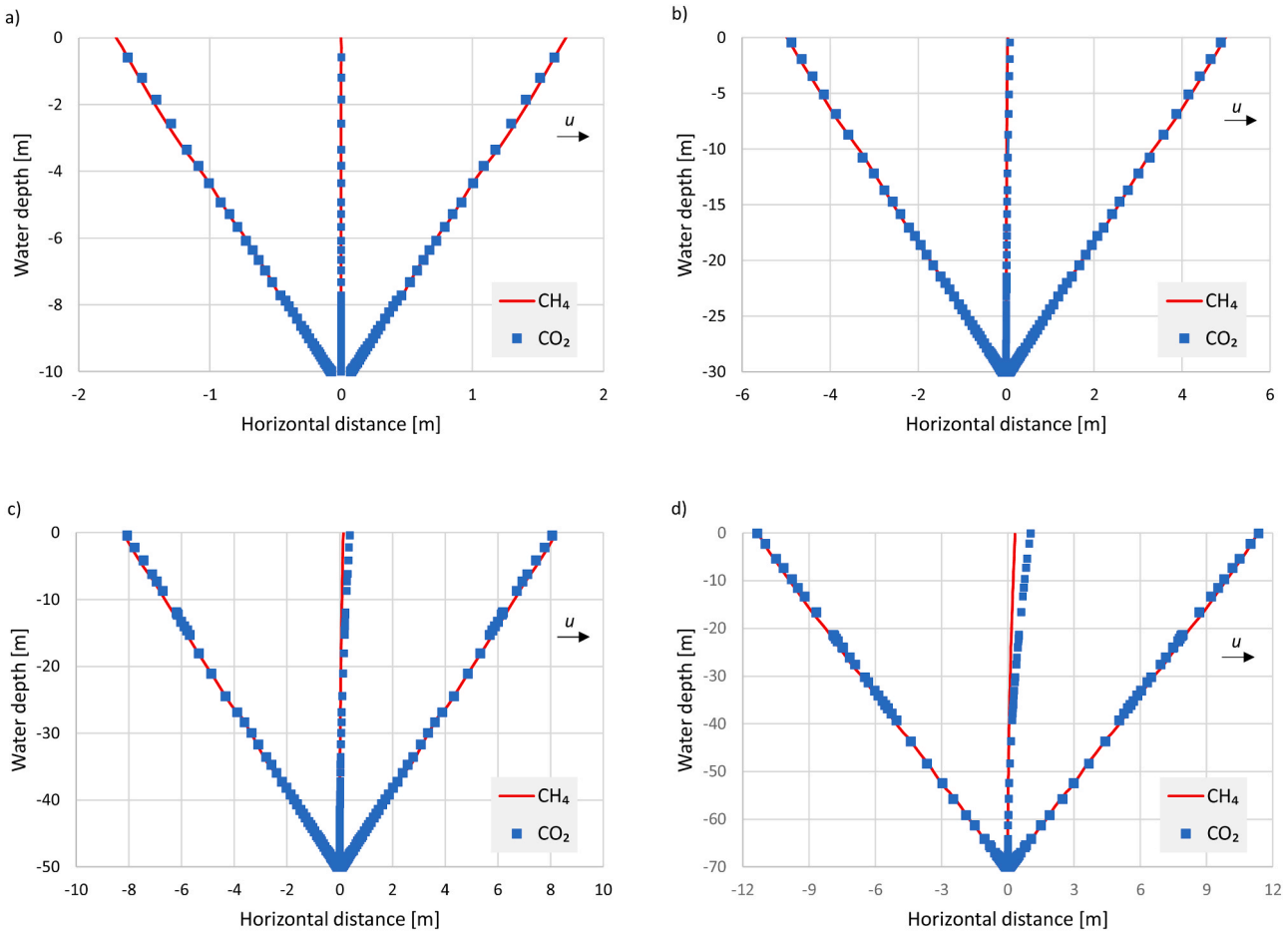

Fig. 7. CH_4 and CO_2 submarine plume profiles and axes for the 200 kg/s blowouts occurring at different seafloor depths: a) − 10 m; b) − 30 m; c) − 50 m; d) − 70 m.

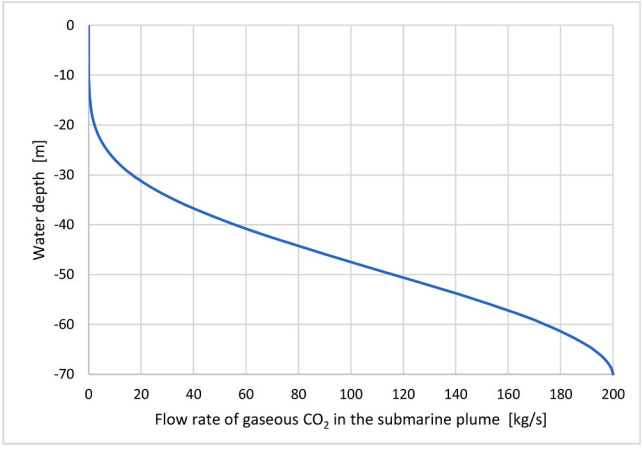

Fig. 8. Flow rate of gaseous CO_2 in the submarine plume as a function of the water depth for the 200 kg/s blowout occurring at a seafloor depth equal to − 70 m.

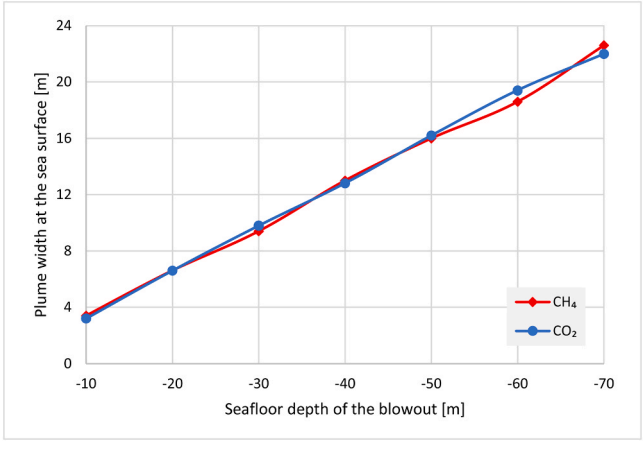

Fig. 9. CH_4 and CO_2 submarine plume width at the sea surface as a function of the seafloor depth of the blowout for the 200 kg/s blowouts.

depth increases from − 10 m to − 20 m, while for blowouts occurring at seafloor depths below − 20 m, the threshold distances decrease constantly with the depth. Actually, when the seafloor depth increases from − 10 m to − 20 m, the reduction in the average velocity of the plume leaving the water column prevails over the decrease in the degassing rate and the increase in the surfacing area, leading to an increase in the threshold distance. However, when the seabed depths rise to values below − 20 m, the strong attenuation of the degassing flow due to the CO_2 absorption in the water column, along with the widening of the outflow section at sea surface, are responsible for the sharp reduction of the threshold distances of the CO_2 plume.

Fig. 12 reports the maximum downwind threshold distances calculated for CH_4 and CO_2 using the PHAST software and the degassing flow rates obtained by the TAMOC simulation for the 200 kg/s blowouts. The results allow a direct comparison of the potential impact areas generated

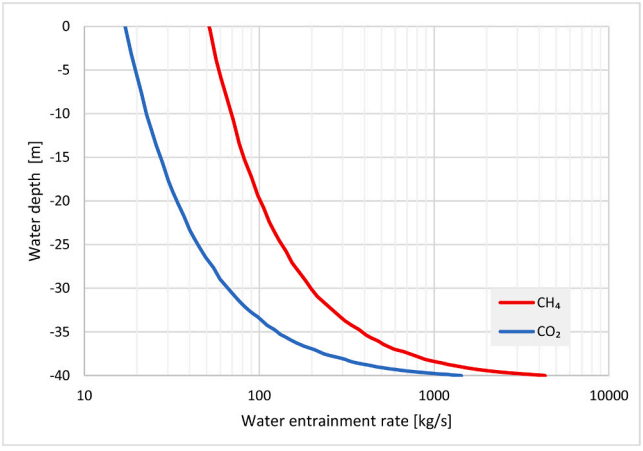

Fig. 10. Water entrainment rate in the submarine plume as a function of the water depth for the 200 kg/s blowouts occurring at a seafloor depth equal to − 40 m.

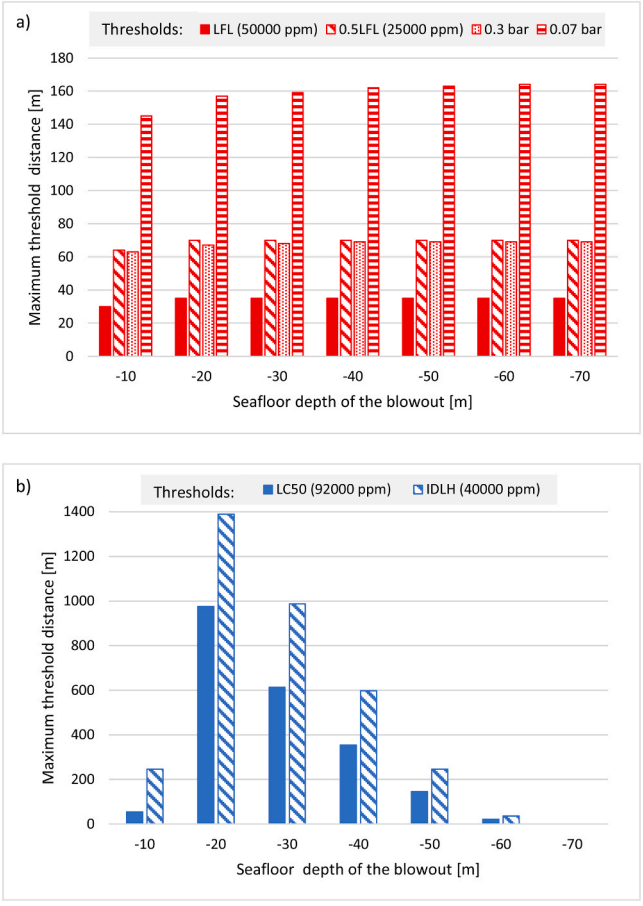

Fig. 11. Maximum downwind threshold distances calculated by the PHAST software for the 200 kg/s blowouts, as a function of the seafloor depth of the blowout for: a) CH_4; b) CO_2.

by the two different substances. Fig. 12 highlights that, for both human health endpoints (i.e., lethal effects and irreversible injuries), CO_2 has much higher threshold distances than CH_4 in the case of blowouts arising at seabed depths in the range − 10 ÷ − 50 m, while for greater seafloor depths the contrary occurs. At high seafloor depths, the CO_2 does not even emerge from the water column. Moreover, as expected, the threshold distances calculated for CH_4 are almost independent from

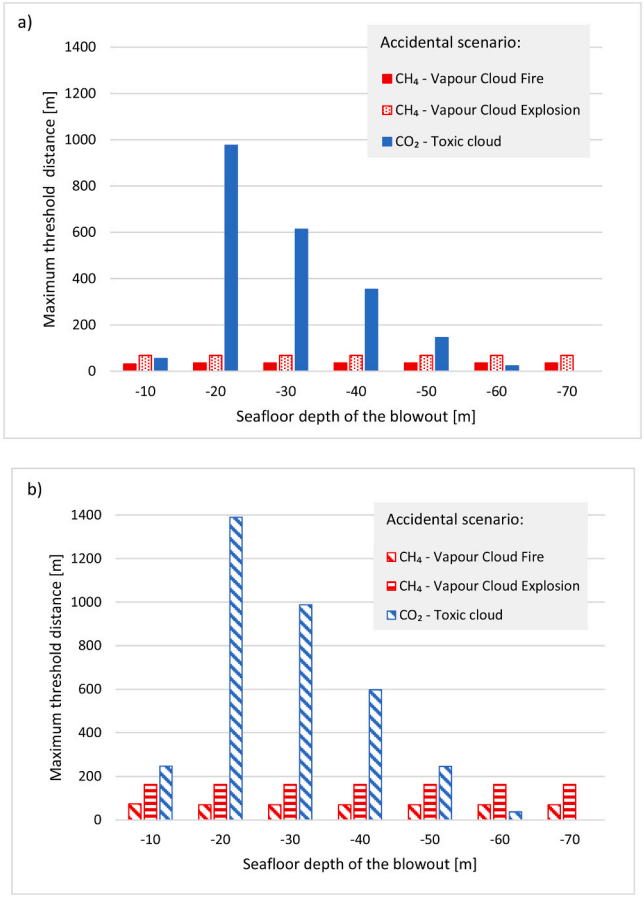

Fig. 12. Maximum downwind threshold distances calculated by the PHAST software for the 200 kg/s blowouts as a function of the seafloor depth corresponding to: a) lethal effects (effect thresholds: 50000 ppm for the CH_4 VCF, 0.3 bar for the CH_4 VCE, 92000 ppm for the CO_2 toxic cloud); b) irreversible injuries (effect thresholds: 25000 ppm for the CH_4 VCF, 0.07 bar for the CH_4 VCE, 40000 ppm for the CO_2 toxic cloud).

the sea depth, since the gaseous CH_4 flow rate is scarcely affected by dissolution in the water column.

Focusing on a seabed depth of − 10 m, at which the two gases have nearly identical degassing flows and surfacing sections, it can be observed that the threshold distances corresponding to lethal effects (see Table 1) are lower for CH_4 (35 m) than for CO_2 (54 m), despite the outflow velocity being higher for CH_4 than for CO_2 (32 m/s versus 13 m/s, respectively) and the lower effect threshold for irreversible injuries of the CH_4 Vapour Cloud Fire (50000 ppm) with respect to the CO_2 toxic cloud (92000 ppm). The difference in the threshold distances derives from the light gas behaviour of CH_4, while CO_2 disperses as a heavy plume.

The distinct behaviour of the two gases can also be inferred from Fig. 13, where the maximum gas plume heights above the sea level are reported for the various seafloor depths considered for the blowouts. These heights are obtained at the plume front for both gases: for CO_2 the plume front is on the sea surface, while for CH_4 it is at a certain height, as shown in Fig. 4. The results reported in Fig. 13 evidence that, in the case of CH_4, the maximum plume height is nearly independent of the seafloor depth, as the threshold distances. Furthermore, the maximum plume heights are much higher for the CH_4 blowouts than for the CO_2 blowouts. In the case of CO_2, the maximum heights depend on the seafloor depth of the blowout, with a trend similar to that of the threshold distances reported in Fig. 11-b).

As mentioned in Section 2, besides the PHAST software, also the EFFECTS and the ALOHA software packages are able to simulate the

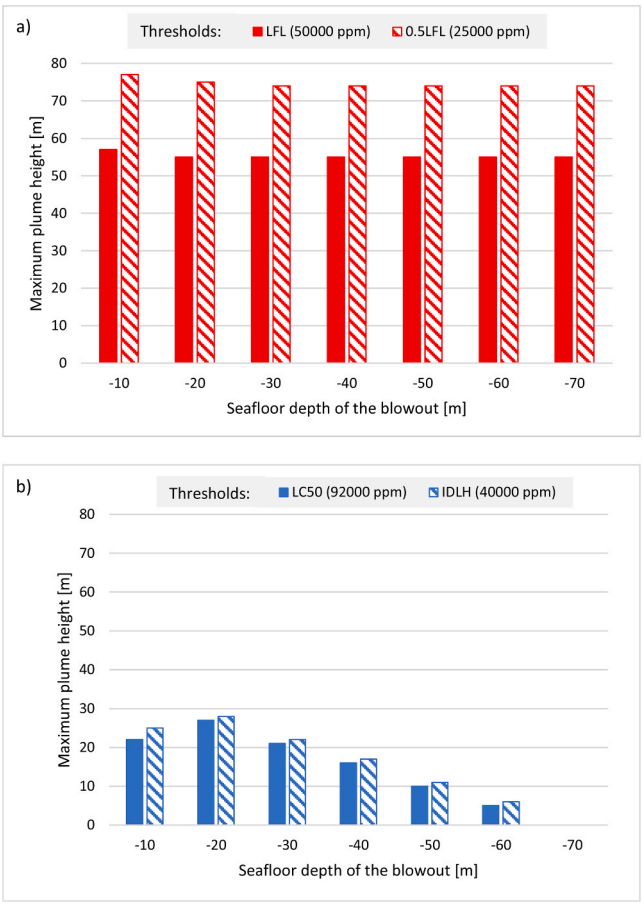

Fig. 13. Maximum plume heights calculated by the PHAST software for the 200 kg/s blowouts as a function of the seafloor depth of the blowout for: a) CH_4; b) CO_2.

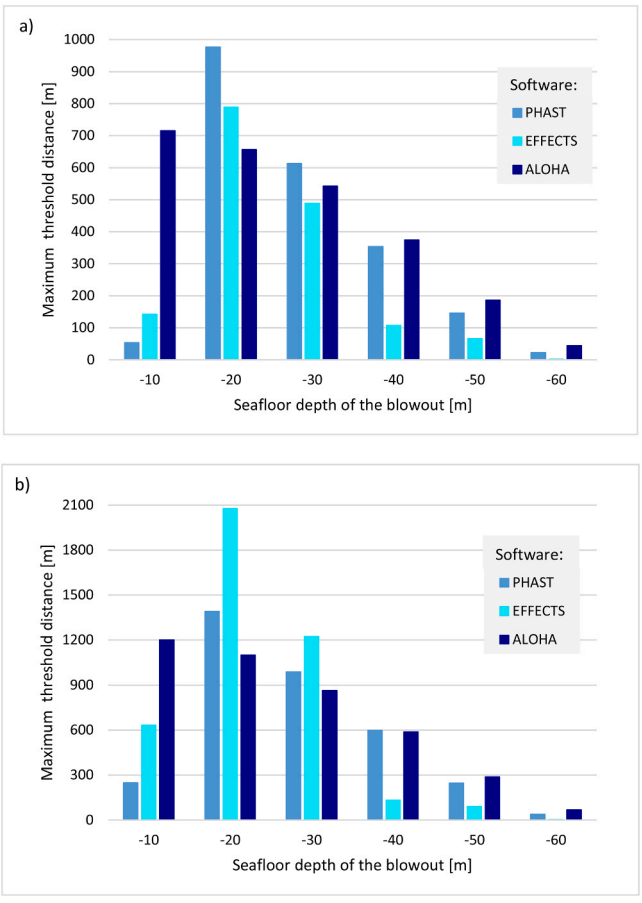

Fig. 14. Maximum downwind threshold distances for the 200 kg/s CO_2 blowout as a function of the seafloor depth of the blowout, corresponding to: a) lethal effects (LC_{50}: 92000 ppm); b) irreversible injuries (IDLH: 40000 ppm).

atmospheric dispersion of heavy gas clouds. Fig. 14 reports a comparison among the results obtained for the 200 kg/s blowouts of CO_2 using these three different software packages. As shown, all the three software codes agree in the trend of the maximum threshold distances with respect to the depth of the seafloor where the blowout is considered to take place. However, differences of up to a factor of 4 are present in the specific results, with greater agreement between the results of the PHAST and the EFFECTS codes, which use similar dispersion models. Actually, the higher discrepancies with the threshold distances obtained with the ALOHA code derive from some limitations of this software. In particular, the ALOHA software is able to consider only point source outflows with negligible velocity. Thus, not considering the outflow speed, it cannot simulate the initial dilution due to the jet release, consequently providing a more conservative estimate of the threshold distances.

5. Discussion

The results of the case studies discussed above provide original and detailed insights concerning the formerly largely unknown impact profile of offshore CO_2 blowouts, for which limited evidence is present in the literature. In particular, the results allow for the first time a comparative assessment among the consequences of CO_2 and those of natural gas offshore blowouts, providing the potential threshold distances for hazardous consequences on human activities on the sea surface caused by subsea blowouts of CH_4 or CO_2.

Moreover, the specific sub-model selected for the water plume dispersion allowed obtaining original results concerning the CO_2 submarine dispersion, where commercial tools usually adopted to estimate the consequences of major accidents fall short in addressing pressure modification to account for the water column effect.

The main outcomes were reported considering the same release rates (200 kg/s) and the same environmental conditions, thus allowing a comparative assessment of the severity of the consequences of CH_4 and CO_2 leakages. Qualitatively similar results were obtained for blowout release rates in the range 100 ÷ 300 kg/s. The main difference caused by the different blowout release rates is that at increasing CO_2 release rates, the seafloor depth below which all the emitted CO_2 is absorbed by the water column increases. This marks a clear difference with respect to natural gas blowouts, since natural gas is not dissolved in the water column.

For scenarios having a blowout rate of 200 kg/s and occurring in extremely shallow waters (i.e., at seafloor depths above − 40 m), the threshold distances of the atmospheric plume are higher for CO_2 than for CH_4. Instead, when the 200 kg/s blowout takes place on deeper sea bottoms, the flow rate of the surfacing CO_2 is substantially reduced by the dissolution of CO_2 in seawater. Thus, for higher seafloor depths, natural gas blowouts determine increasingly higher threshold distances than CO_2.

The case studies examined were analysed by applying integral models to describe both the submarine plume and the atmospheric dispersion of the gas emerging from the water column. Indeed, integral models do not need an accurate description of the offshore structures that may be affected by the atmospheric plume. This feature of integral models, along with the low requirement of computational resources, makes them preferable for a first screening of the threshold distances. The findings provided by integral models can be very useful in defining

the computational domain of CFD models, which may be applied if more detailed analyses are needed. Therefore, CFD modelling, applied to both submarine and atmospheric dispersion, may represents an extension of the analysis reported in Section 4.

The presence of anthropogenic activities on the sea surface (e.g., offshore installations and ships), along with the protracted duration of the blowout, make the ignition of natural gas clouds highly probable. Furthermore, similar frequencies of occurrence are expected for natural gas and CO_2 blowouts. Thus, the considerations concerning the effects of the natural gas and CO_2 blowouts can be extended to risk, which is a function of both the occurrence frequencies and the effects of accident scenarios. Clearly enough, the proposed methodology is able to support the quantitative risk assessment (QRA) to humans deriving from subsea blowouts. This is particularly important from the perspective of the reuse of depleted gas reservoirs for the geological storage of CO_2 in shallow waters, as in the case of the gas fields just off the coastline, where non-negligible risks, requiring appropriate management, may affect human activities.

However, when considering the possible targets of natural gas and CO_2 blowouts in a risk assessment framework, it should also be remarked that on the one hand, asset damage should be considered in the case of natural gas clouds, that have the potential to harm ships and offshore facilities engulfed in the atmospheric plume. On the other hand, the low solubility of natural gas limits the threat of natural gas blowouts to the marine environment. Differently, the acidification of the seawater caused by the dissolution of CO_2 can damage the biota present in the water column and on the seafloor. Hence, to build up a thorough picture of the risk associated to the geological CO_2 storage, it is also necessary to assess the effects that CO_2 releases cause on the environment. It has also to be highlighted that the methodology proposed only focuses on blowouts from exploitation or injection wells. Other types of submarine leakage events may affect CCUS projects and need to be considered in a wider risk assessment context: e.g., spills from abandoned wells, from fractures and faults, from cap rock hydro-fractures, and from sealines.

Finally, it is crucial to emphasize that the methodology developed in the present study is also capable of solidly supporting emergency planning in offshore structures. Actually, comparing the maximum plume heights (e.g., see the results reported in Fig. 13) with the height above the sea level (ASL) of offshore platforms, it is possible to understand how hazardous concentrations may affect these installations. As an example, when considering the Adriatic Sea, most of the existing offshore platforms for gas exploitation have a height from 15 m to 65 m ASL, depending on the number of decks (usually 1 to 3) (WebGIS UNMIG, 2023). Specifically, level deck 1 is usually at least 15 m ASL, while level 3 deck is never higher than 65 m ASL. Considering the CH_4 plume heights shown in Fig. 13, all scenarios having a blowout rate of 200 kg/s can potentially cause dangerous concentrations on such installations. Differently, only the 200 kg/s CO_2 blowouts occurring at a seabed depth between − 10 m and − 40 m can determine hazardous concentrations on such structures, and only on the decks at heights below 30 m ASL. In the specific scenario considered, the plumes deriving from CO_2 blowouts occurring on deeper seafloors are not even able to affect the lower deck of these facilities. Although such results are specific of the case studies examined, and considering higher blowout rates may increase the maximum plume height, the qualitative trend of the hazardous concentrations is unaffected by the blowout rate. Thus, the higher decks of the offshore installations are affected by lower concentrations of CO_2, irrespectively of the blowout rate. This observation is certainly useful in emergency planning for CO_2 injection facilities in shallow waters, where sheltering in the upper decks should be usually preferred to mustering on the jetty of the rig at the sea level.

6. Conclusions

The innovative methodology developed for the evaluation of the potential impact on humans of gaseous submarine releases of CO_2 allows a comprehensive and straightforward assessment of the threshold distances at the sea surface for CO_2 blowouts. The novel procedure developed is based on an integrated and flexible framework, where three independent sub-models are linked in order to simulate both the plume of gas bubbles in the water column and the atmospheric dispersion of the gas emerging into the air. Case-specific damage distances are obtained from the application of the method, taking into account the most important factors on which these distances depend.

The notional case studies explored evidenced the relevance of the consequences of blowouts on the sea surface, considering both the flammability hazards of natural gas and the toxic effects of CO_2. Depending on the seafloor depth at which the blowouts occur, the order of magnitude of the threshold distances for lethal effects on humans may range from 100 m to 1000 m. Thus, the outcomes of the case studies highlight the severity of the potential damage of CO_2 subsea blowouts to human activities on the sea surface, which has to be considered in addition to the damage to the marine environment.

The modelling approach developed paves the way for a systematic quantitative risk assessment of such hazards in both conventional natural gas exploitation and innovative offshore CCUS projects. Its ability to outline the risk profiles of CO_2, for which limited experience is presently available, and natural gas, which is characterized by a well-known and widely recognized hazard, makes it a frontrunner in addressing future challenges in the context of the risk management of CCUS projects.

Declaration of Competing Interest

The authors declare that they have no known competing financial interests or personal relationships that could have appeared to influence the work reported in this paper.

References

[dataset] DNV, 2017. The Worldwide Offshore Accident Databank (WOAD).
[dataset] SINTEF, 2021. SINTEF offshore-blowout-database [WWW Document]. URL ⟨https://www.sintef.no/en/projects/2021/sintef-offshore-blowout-database/⟩.
Amir Rashidi, M.R., Dabbi, E.P., Abu Bakar, Z.A., Shahir Misnan, M., Pedersen, C., Wong, K.Y., Sallehud-Din, T.T.M., Azim Shamsudin, M., Wo, S., 2020. A field case study of modelling the environmental fate of leaked CO_2 gas in the marine environment for carbon capture and storage CCS. in: Society of Petroleum Engineers. SPE Asia Pacific Oil and Gas Conference and Exhibition 2020, APOG 2020. Society of Petroleum Engineers,, pp. 1–16. https://doi.org/10.2118/202394-MS.
Ansys, 2023a. Ansys Fluent.
Ansys, 2023b. Ansys CFX.
Artegiani, A., Bregant, D., Paschini, E., Pinardi, N., Raicich, F., Russo, A., 1997. The adriatic sea general circulation. Part I: Air-sea. Interact. Water Mass Struct. J. Phys. Oceano 27, 1492–1514. https://doi.org/10.1175/1520-0485(1997)027<1492:TASGCP>2.0.CO;2.
Beegle-Krause, C., Lynch, W., 2005. Combining modeling with response in potential deep well blowout: lessons learned from thunder horse, in: Proceedings of IOSC 2005 - International Oil Spill Conference. Miami Beach FL, USA, pp. 1–6.
BEIS, 2021. Net Zero Teesside and Northern Endurance Partnership Technology Plan. London.
Blackford, J., Jones, N., Proctor, R., Holt, J., Widdicombe, S., Lowe, D., Rees, A., 2009. An initial assessment of the potential environmental impact of CO_2 escape from marine carbon capture and storage systems. J. Power Energy, Part A Proc. Inst. Mech. Eng. 223, 269–280. https://doi.org/10.1243/09576509JPE623.
Blackford, J., Haeckel, M., Wallmann, K., 2012. Report on range of long-term scenarios to be simulated. ECO_2 research project "Sub-seabed CO_2 Storage: Impact on Marine Ecosystems", WP12 - deliverable. ECO2 Proj. Off. D12.2. https://doi.org/10.3289/ECO2_D12.2.
Blackford, J., Alendal, G., Avlesen, H., Brereton, A., Cazenave, P.W., Chen, B., Dewar, M., Holt, J., Phelps, J., 2020. Impact and detectability of hypothetical CCS offshore seep scenarios as an aid to storage assurance and risk assessment. Int. J. Greenh. Gas. Control 95, 1–11. https://doi.org/10.1016/j.ijggc.2019.102949.
Blackford, J.C., Torres, R., Cazanave, P., Artioli, Y., 2013. Modelling dispersion of CO_2 plumes in sea water as an aid to monitoring and understanding ecological impact. Energy Procedia 37, 3379–3386. https://doi.org/10.1016/J.EGYPRO.2013.06.226.
Bolaños, R., Tornfeldt Sørensen, J.V., Benetazzo, A., Carniel, S., Sclavo, M., 2014. Modelling ocean currents in the northern Adriatic Sea. Cont. Shelf Res. 87, 54–72. https://doi.org/10.1016/J.CSR.2014.03.009.
Chadwick, A., Eiken, O., 2013. Offshore CO2 storage Sleipner natural gas field beneath the North Sea, in: Gluyas, J. and Mathias, S. (Ed.), Geological Storage of Carbon Dioxide (CO2) - Geoscience, Technologies, Environmental Aspects and Legal Frameworks. Woodhead Publishing, Sawston (UK), pp. 1–23.

ClimateWise, 2012. Managing liabilities of european Carbon Capture and Storage. Cambridge.
Cloete, S., Olsen, J.E., Skjetne, P., 2009. CFD modeling of plume and free surface behavior resulting from a sub-sea gas release. Appl. Ocean Res. 31, 220–225. https://doi.org/10.1016/j.apor.2009.09.005.
Crounse, B.C., 2000. Modeling buoyant droplet plumes in a stratified environment. Massachusetts Institute of Technology.
D.M. 09.05.2001, 2001. Requisiti minimi di sicurezza in materia di pianificazione urbanistica e territoriale per le zone interessate da stabilimenti a rischio di incidente rilevante. Gazz. Uff. della Repubb. Ital (in Italian).
Dewar, M., Chen, B., Evgeniy, Y., Avlesen, H., Alendal, G., Ali, A., Vielstädte, L., 2014. Technical report on verified and validated application of droplet/bubble plume-, geochemical- and general flow- models. ECO2 research project "Sub-seabed CO2 Storage: Impact on Marine Ecosystems", WP3 - deliverable D3.3.
Directive 2009/31/EC, 2009. DIRECTIVE 2009/31/EC OF THE EUROPEAN PARLIAMENT AND OF THE COUNCIL of 23 April 2009 on the geological storage of carbon dioxide and amending Council Directive 85/337/EEC, European Parliament and Council Directives 2000/60/EC, 2001/80/EC, 2004/35/EC, 2006/. Off. J. Eur. Union.
Dissanayake, A.L., Gros, J., Socolofsky, S.A., 2018. Integral models for bubble, droplet, and multiphase plume dynamics in stratification and crossflow. Environ. Fluid Mech. 18, 1167–1202. https://doi.org/10.1007/s10652-018-9591-y.
Dissanayake, A.L., Nordam, T., Gros, J., 2021. Simulations of subsea CO2 leakage scenarios, in: Press, S.A. (Ed.), Proc., Trondheim Conf. on CO2 Capture, Transport and Storage. Trondheim, Norway, pp. 384–389.
DNV, 2023a. KFX.
DNV, 2023b. PHAST.
EC, 2011. Implement. Dir. 2009/31/EC Geol. Storage Carbon Dioxide - Guid. Doc. 1: CO_2 Storage Life Cycle Risk Manag. Framew. https://doi.org/10.2834/9801.
Engineering Toolboox, 2023. Gas densities [WWW Document]. URL ⟨https://www.engineeringtoolbox.com/gas-density-d_158.html⟩ (accessed 9.22.23).
ENI, 2020. Rapporto locale di sostenibilità - Eni a Ravenna 2020. Roma (in Italian).
Equinor, 2019a. Northern Lights Project Concept report, Document RE-PM673–00001. Stavanger.
Equinor, 2019b. Miljørisiko for EL001, Northern Lights, mottak og permanent lagring av CO2. Stavanger (in Norwegian).
ETIP ZEP, 2019. CO2 storage safety in the North Sea: implications of the CO2 storage directive.
Fluidyn, 2023. The PANACHE CFD code.
Gant, S.E., Narasimhamurthy, V.D., Skjold, T., Jamois, D., Proust, C., 2014. Evaluation of multi-phase atmospheric dispersion models for application to Carbon Capture and Storage. J. Loss Prev. Process Ind. 32, 286–298. https://doi.org/10.1016/J.JLP.2014.09.014.
W.M.S. GEBCO [WWW Document], 2023. URL ⟨https://www.gebco.net/data_and_products/gebco_web_services/web_map_service/⟩.
Geng, Z., Li, X., Chen, G., Zhu, H., Jiang, S., 2021. Experimental and numerical study on gas release and dispersion from underwater soil. Process Saf. Environ. Prot. 149, 11–21. https://doi.org/10.1016/j.psep.2020.09.065.
Gexcon, 2023a. FLACS-CFD.
Gexcon, 2023b. EFFECTS.
Glade, H., Al-Rawajfeh, A.E., 2008. Modeling of CO_2 release and the carbonate system in multiple-effect distillers. Desalination 222, 605–625. https://doi.org/10.1016/J.DESAL.2007.02.069.
Gros, J., Socolofsky, S.A., Dissanayake, A.L., Jun, I., Zhao, L., Boufadel, M.C., Reddy, C. M., Arey, J.S., 2017. Petroleum dynamics in the sea and influence of subsea dispersant injection during Deepwater Horizon. Environ. Sci. 114, 10065–10070. https://doi.org/10.1073/PNAS.1612518114/SUPPL_FILE/PNAS.1612518114.SAPP.PDF.
Gros, J., Dissanayake, A.L., Daniels, M.M., Barker, C.H., Lehr, W., Socolofsky, S.A., 2018. Oil spill modeling in deep waters: Estimation of pseudo-component properties for cubic equations of state from distillation data. Mar. Pollut. Bull. 137, 627–637. https://doi.org/10.1016/J.MARPOLBUL.2018.10.047.
Gros, J., Schmidt, M., Dale, A.W., Linke, P., Vielstädte, L., Bigalke, N., Haeckel, M., Wallmann, K., Sommer, S., 2019. Simulating and Quantifying Multiple Natural Subsea CO_2 Seeps at Panarea Island (Aeolian Islands, Italy) as a Proxy for Potential Leakage from Subseabed Carbon Storage Sites. Environ. Sci. Technol. 53, 10258–10268. https://doi.org/10.1021/acs.est.9b02131.
Harper, P., Wilday, J., Bilio, M., 2011. Assessment of the major hazard potential of carbon dioxide (CO2) 1–28.
Haynes, W.M., 2014. Handbook of Chemistry and Physics (95th 2014–2015 edition), Journal of the American Pharmaceutical Association.
Holand, P., 1997. Offshore Blowouts: Causes and Control. Gulf Publishing Company, Houston (USA).
Hoteit, H., Fahs, M., Soltanian, M.R., 2019. Assessment of CO_2 injectivity during sequestration in depleted gas reservoirs. Geosciences 9, 199. https://doi.org/10.3390/GEOSCIENCES9050199.
HSE, 2009. Comparison of risks from carbon dioxide and natural gas pipelines, research report RR749. Bootle (UK).
Hueschen, M.A., 2010. Can bubbles sink ships? Am. J. Phys. 78, 139–141. https://doi.org/10.1119/1.3263819.
IEA, 2020. Energy Technology Perspectives 2020 - Special Report on Carbon Capture Utilisation and Storage. Paris. https://doi.org/10.1787/208b66f4-en.
IEA, 2021. World Energy Outlook 2021, World Energy Outlook. OECD, Paris. https://doi.org/10.1787/14fcb638-en.
IOGP, 2019. Risk Assessment Data Directory - Blowout Frequencies, report 434–02. London.
IPCC, 2005. IPCC Special Report on Carbon Dioxide Capture and Storage, 1st ed. Cambridge University Press, Cambridge, United Kingdom and NewYork, NY, USA.
Jewell, S., Senior, B., 2012. CO2 Storage Liabilities in the North Sea - An Assessment of Risks and Financial Consequences. UK.
Jones, D.G., Beaubien, S.E., Blackford, J.C., Foekema, E.M., Lions, J., De Vittor, C., West, J.M., Widdicombe, S., Hauton, C., Queirós, A.M., 2015. Developments since 2005 in understanding potential environmental impacts of CO_2 leakage from geological storage. Int. J. Greenh. Gas. Control 40, 350–377. https://doi.org/10.1016/J.IJGGC.2015.05.032.
Jordan, P.D., Benson, S.M., 2008. Well blowout rates and consequences in California Oil and Gas District 4 from 1991 to 2005: Implications for geological storage of carbon dioxide. Environ. Geol. 57, 1103–1123. https://doi.org/10.1007/S00254-008-1403-0.
Kongsberg Digital, 2023. LedaFlow.
Koornneef, J., Spruijt, M., Molag, M., Ramírez, A., Turkenburg, W., Faaij, A., 2010. Quantitative risk assessment of CO_2 transport by pipelines-A review of uncertainties and their impacts. J. Hazard. Mater. 177, 12–27. https://doi.org/10.1016/j.jhazmat.2009.11.068.
Li, X., Wang, J., 2023. Modelling underwater dispersion of gas released from seabed soil considering current and wave. Process Saf. Environ. Prot. 171, 260–271. https://doi.org/10.1016/j.psep.2023.01.030.
Li, X., Chen, G., Zhang, R., Zhu, H., Fu, J., 2018a. Simulation and assessment of underwater gas release and dispersion from subsea gas pipelines leak. Process Saf. Environ. Prot. 119, 46–57. https://doi.org/10.1016/J.PSEP.2018.07.015.
Li, X., Chen, G., Zhu, H., Xu, C., 2018b. Gas dispersion and deflagration above sea from subsea release and its impact on offshore platform. Ocean Eng. 163, 157–168. https://doi.org/10.1016/j.oceaneng.2018.05.059.
Li, X., Chen, G., Khan, F., 2019. Analysis of underwater gas release and dispersion behavior to assess subsea safety risk. J. Hazard. Mater. 367, 676–685. https://doi.org/10.1016/j.jhazmat.2019.01.015.
Lian, Z., Li, F., He, X., Chen, J., Yu, R.C., 2022. Rising CO_2 will increase toxicity of marine dinoflagellate Alexandrium minutum. J. Hazard. Mater. 431, 128627 https://doi.org/10.1016/j.jhazmat.2022.128627.
OpenC.F.D. Ltd, 2023. OpenFOAM.
Mannan, S., 2012. Lees' Loss Prevention in the Process Industries: Hazard Identification, Assessment And Control: Fourth Edition, 4th ed. Butterworth-Heinemann. https://doi.org/10.1016/C2009–0-24104–3.
Meteo Areonautica Militare [W.W.W. Document], 2023. URL ⟨https://clima.meteoam.it/⟩ (accessed 5.11.23).
NIOSH, 2007. Pocket Guide for Chemical Hazards, publication n° 2005–149.
Norwegian Oil and Gas Association, 2021. Guidance on calculating blowout rates and duration for use in environmental risk analyses. Stavanger.
Oldenburg, C.M., Pan, L., 2019. Simulation study comparing offshore versus onshore CO_2 well blowouts. : Offshore Technol. Conf. OnePetro, Houst., Tex., Usa. https://doi.org/10.4043/29461-MS.
Oldenburg, C.M., Pan, L., 2020. Major CO_2 blowouts from offshore wells are strongly attenuated in water deeper than 50 m. Greenh. Gases Sci. Technol. 10, 15–31. https://doi.org/10.1002/GHG.1943.
Oldenburg, C.M., Zhang, Y., 2022. Downwind dispersion of CO_2 from a major subsea blowout in shallow offshore waters. Greenh. Gases Sci. Technol. 12, 321–331. https://doi.org/10.1002/GHG.2144.
Olsen, J.E., Skjetne, P., 2016. Current understanding of subsea gas release: a review. Can. J. Chem. Eng. 94, 209–219. https://doi.org/10.1002/cjce.22345.
Olsen, J.E., Skjetne, P., 2020. Summarizing an Eulerian–Lagrangian model for subsea gas release and comparing release of CO_2 with CH4. Appl. Math. Model. 79, 672–684. https://doi.org/10.1016/J.APM.2019.10.057.
Pan, L., Oldenburg, C.M., 2014. T2Well—An integrated wellbore–reservoir simulator. Comput. Geosci. 65, 46–55. https://doi.org/10.1016/J.CAGEO.2013.06.005.
Papanikolaou, E., Heitsch, M., Baraldi, D., 2011. Validation of a numerical code for the simulation of a short-term CO_2 release in an open environment: Effect of wind conditions and obstacles. J. Hazard. Mater. 190, 268–275. https://doi.org/10.1016/j.jhazmat.2011.03.041.
Pham, L.H.H.P., Rusli, R., Shariff, A.M., Khan, F., 2020. Dispersion of carbon dioxide bubble release from shallow subsea carbon dioxide storage to seawater. Cont. Shelf Res. 196, 104075 https://doi.org/10.1016/J.CSR.2020.104075.
Porse, S.L., Wade, S., Hovorka, S.D., 2014. Can we treat CO_2 well blowouts like routine plumbing problems? A study of the incidence, impact, and perception of loss of well control. Energy Procedia 63, 7149–7161. https://doi.org/10.1016/J.EGYPRO.2014.11.751.
Roberts, J.J., Stalker, L., 2020. What have we learnt from CO_2 release field experiments and what are the gaps for the future? Earth-Sci. Rev. 209 https://doi.org/10.1016/j.earscirev.2019.102939.
Ruppel, C., Boswell, R., Jones, E., 2008. Scientific results from Gulf of Mexico Gas Hydrates Joint Industry Project Leg 1 drilling: Introduction and overview. Mar. Pet. Geol. 25, 819–829. https://doi.org/10.1016/J.MARPETGEO.2008.02.007.
Schlumberger, 2023. Drillbench Blowout Control software.
Sellami, N., Dewar, M., Stahl, H., Chen, B., 2015. Dynamics of rising CO_2 bubble plumes in the QICS field experiment: Part 1 – The experiment. Int. J. Greenh. Gas. Control 38, 44–51. https://doi.org/10.1016/J.IJGGC.2015.02.011.
Sherpa Consulting, 2015. Dispersion Modelling Techniques for Carbon Dioxide Pipelines in Australia. Document n. 20873-RP-001.
Socolofsky, S.A., Bhaumik, T., 2008. Dissolution of Direct Ocean Carbon Sequestration Plumes Using an Integral Model Approach. J. Hydraul. Eng. 134, 1570–1578. https://doi.org/10.1061/(ASCE)0733-9429(2008)134:11(1570).

Socolofsky, S.A., Bhaumik, T., Seol, D.G., 2008. Double-plume integral models for near-field mixing in multiphase plumes. J. Hydraul. Eng. 134, 772–783. https://doi.org/10.1061/(ASCE)0733-9429(2008)134:6(772).

Socolofsky, S.A., Dissanayake, A.L., Jun, I., Gros, J., Samuel Arey, J., Reddy, C.M., 2015. Texas A&M Oilspill Calculator (TAMOC): Modeling Suite for Subsea Spills, in: Proceedings of the 38th AMOP Technical Seminar on Environmental Contamination and Response. pp. 153–168.

Sponge, J., 1999. A guide to quantitative risk assessment for offshore installations. CMPT - Center for Marine and Petroleum Technology publication 99/100, UK.

Sun, Y., Cao, X., Liang, F., Bian, J., 2020. Investigation on underwater gas leakage and dispersion behaviors based on coupled Eulerian-Lagrangian CFD model. Process Saf. Environ. Prot. 136, 268–279. https://doi.org/10.1016/j.psep.2020.01.034.

TAMOC, 2023. Texas A&M Oilspill Calculator.

The Netherlands Organization of Applied Scientific Research, 2005. Methods for the calculation of physical effects (yellow book). Publ. Ser. Danger. Subst. 870.

Ulfsnes, A., Møskeland, T., Brooks, L., 2013. Report on environmental risks associated to CO2 storage at Sleipner. ECO2 research project "Sub-seabed CO2 Storage: Impact on Marine Ecosystems", WP5 - deliverable D5.1.

US EPA, 2023. ALOHA.

Wang, B., Socolofsky, S.A., Lai, C.C.K., Adams, E.E., Boufadel, M.C., 2018. Behavior and dynamics of bubble breakup in gas pipeline leaks and accidental subsea oil well blowouts. Mar. Pollut. Bull. 131, 72–86. https://doi.org/10.1016/j.marpolbul.2018.03.053.

WebGIS UNMIG [W.W.W. Document], 2023. URL ⟨https://unmig.mite.gov.it/⟩ (accessed 5.11.23).

Weiss, R.F., 1974. Carbon dioxide in water and seawater: the solubility of a non-ideal gas. Mar. Chem. 2, 203–215. https://doi.org/10.1016/0304-4203(74)90015-2.

Widdicombe, S., Dashfield, S.L., McNeill, C.L., Needham, H.R., Beesley, A., McEvoy, A., Øxnevad, S., Clarke, K.R., Berge, J.A., 2009. Effects of CO_2 induced seawater acidification on infaunal diversity and sediment nutrient fluxes. Mar. Ecol. Prog. Ser. 379, 59–75. https://doi.org/10.3354/MEPS07894.

Widdicombe, S., McNeill, C.L., Stahl, H., Taylor, P., Queirós, A.M., Nunes, J., Tait, K., 2015. Impact of sub-seabed CO_2 leakage on macrobenthic community structure and diversity. Int. J. Greenh. Gas. Control 38, 182–192. https://doi.org/10.1016/J.IJGGC.2015.01.003.

Witlox, H.W.M., Fernandez, M., Harper, M., Stene, J., 2017. Modelling and validation of atmopsheric expansion and near-field dispersion for pressurised vapour or two-phase releases. J. Loss Prev. Process Ind. 48, 331–344. https://doi.org/10.1016/j.jlp.2017.05.005.

Xing, J., Liu, Z., Huang, P., Feng, C., Zhou, Y., Zhang, D., Wang, F., 2013. Experimental and numerical study of the dispersion of carbon dioxide plume, 40–48 J. Hazard. Mater. 256–257. https://doi.org/10.1016/j.jhazmat.2013.03.066.

Yamamoto, S., Alcauskas, J.B., Crozier, T.E., 1976. Solubility of methane in distilled water and seawater. J. Chem. Eng. Data 21, 78–80. https://doi.org/10.1021/JE60068A029/ASSET/JE60068A029.FP.PNG_V03.

Zhang, Y., Oldenburg, C.M., Pan, L., 2016. Fast estimation of dense gas dispersion from multiple continuous CO_2 surface leakage sources for risk assessment. Int. J. Greenh. Gas Control 49, 323–329. https://doi.org/10.1016/J.IJGGC.2016.03.002.